6th International Conference on Microelectronics and Computer Science, Chişinău, Republic of Moldova, October 1-3, 2009

Light Induced Modification of the Refractive Index of Sb_2Se_3:Sn Thin Films

M.A.IOVU, D.V.HAREA, O.IASENIUC, E.P.COLOMEICO, A.MESHALKIN, M.S.IOVU
Institute of Applied Physics of the Academy of Sciences of Moldova
Str. Academiei 5, MD-2028 Chisinau, R. Moldova
E-mail: maria.iovu@phys.asm.md

Abstract. *The optical properties of chalcogenide glasses present a great scientific interest for the establishment of the general legitimacy of interaction of the optical irradiation with the amorphous solids, as well as a practical interest. The effect of light-induced photostructural transformations in amorphous chalcogenides films have been initiated many applications of amorphous material in photonics and optoelectronics, especially as inorganic photo-resists for sub-micron technology. The optical parameters of amorphous Sb_2Se_3 and Sb_2Se_3:Sn_x (x=0.01, 0.5, 10 at. Sn %) prepared by vacuum evaporation on glass substrates was determined from transmission spectra. The band gap was found to be E_g=1.30 eV for amorphous Sb_2Se_3 and decrease with increasing of tin concentration up to E_g=1.0 eV for Sb_2Se_3:$Sn_{10.0}$. For determination of the refractive index the approximation method proposed by Valeev was used. The maximum modifications of the refractive index under the light irradiation $\Delta n \sim 0.20$ occur for the composition Sb_2Se_3:$Sn_{0.01}$. That allows us to conclude that doping of amorphous Sb_2Se_3 films with small concentrations of tin initiate the photostructural transformations under the light irradiation, and make these materials suitable for registration of optical and holographic information.*

Keywords: Amorphous films, Optical absorption, Refractive index, Photoinduced phenomena

1. Introduction

The effect of light-induced photostructural transformations is characteristic for many amorphous chalcogenides films, and have been initiated a lot of applications of amorphous material in photonics and optoelectronics, especially as inorganic photo-resists for sub-micron technology [1]. Special interest for the applications of chalcogenide amorphous films is connected with doping with metal impurities, which alter optical, photoelectrical and transport properties of the host material [2-4]. At the same time doping of chalcogenide films by tin impurities assist in stabilizing the glassy matrix with respect to light exposure and thermal treatment [5,6].

The crystalline antimony selenide (Sb_2Se_3) is a layer-structured semiconductor with melting temperature T_g=590 ^{0}C [7]. The basic structural units are the $SbSe_{3/2}$-pyramides. Sb_2Se_3 is a direct band gap semiconductor with orthorhombic crystal structure, and present a greet interest due to its switching effects and its potential applications in photovoltaic [8-10]. As was found in [11], for the thermally evaporated α-$(Sb_2Se_3)_{100-x}Sn_x$ thin films the thermally activation energy decreases, while the optical band gap first increase (up to x=1) and then decrease, with the increase in Sn content. These behaviours was explained taking into account the structural modifications induced by the incorporation of Sn impurities in the host material. The thermal activation energy ΔE_a for pure α-Sb_2Se_3 was estimated as ΔE_a=0.42 eV [12]. In [13] was reported the results of preparation on the base of Sb_2Se_3 nanoribbons, and can be used for fabrication of high sensitive sensors due to the fact that the surface to volume ration (*S/V*) is very high. The optical band gap determined from optical measurement for α-Sb_2Se_3 was estimated E_g=1.15 eV [13], and E_g=1.18 eV [14]. For technological applications in solar energy conversion, and also for a wide range of optical nanodevices operating in the near infrared region of the spectrum was proposed the low-cost $Sb_2Se_{3-x}S_x$ nanotubes [14]. Polycrystalline and amorphous Sb_2Se_3 films extend the possibilities of its application in photonics and optoelectronics [15,16]. The addition of third elemental impurity such as Sn in amorphous Sb_2Se_3 films can provide a pronounced effect on electrical, transport properties, optical and photoinduced phenomena [17,18]. For the Sb_2S_3, Sb_2Se_3 and Sb_2Te_3 also was demonstrated the amorphous-to-crystalline phase change induced by CW Ar^+ laser [19]. The photo-thermal processes are found to be responsible for the phase change in all antimony chalcogenides. It was found that the more potential candidate for use as the worm kind of storage devices is the Sb_2Se_3 films, having a minimum threshold power (about 100 W/cm^2. The chalcogenide glasses containing antimony also were investigated in order to obtain chemical micro sensors and sensitive membranes for the detection of Cd^{2+} and Cu^{2+} ions in solutions [20,21]. In this paper are presented the experimental results of optical transmission spectra of thermally evaporated thin films (thickness ~1 μm) of Sb_2Se_3 and Sb_2Se_3:Sn_x (x=0.01, 0.5, 10 at.%). The refractive index changes for different

amorphous Sb_2Se_3:Sn_x films under the light exposure and heat treatment is estimated.

1. Experimental

The Sb_2Se_3 and Sb_2Se_3:Sn_x (x=0.01, 0.5 and 10 at.% Sn) were fabricated by "flash" thermal evaporation in vacuum (p=10^{-5} Torr) of the initial synthesized material onto the clean glass substrates. The thickness of the films was about d~1 μm. For optical transmission a UV/VIS (300÷800 nm) and 61 NIR (800÷3500 nm) Specord's CARLZEISS Jena production were used.

The influence of the light exposure on the optical transmission was examined by illumination of the samples during 1 hour by light with the intensity F=50000 Lux. The thermal treating effect was examined by annealing of a part of the films in vacuum at T_{ann}=100 ^oC during one hour. After the annealing and light exposure the optical transmission was registered in the same manner.

2. Results and discussion

The microscopically studies show that all as-deposited Sb_2Se_3 are amorphous. The heat treatment and light exposure modify the morphology, some crystalline clusters appear, which are distributed non-uniformly in the sample. The number and the size of clusters after the heat treatment and light exposure increase with the increasing of the concentration of Sn impurity in Sb_2Se_3 films.

Fig.1 shows the transmission spectra for as-deposited amorphous Sb_2Se_3 thin films. The transmission spectra for Sb_2Se_3:$Sn_{0.01}$ and Sb_2Se_3:$Sn_{0.5}$ and Sb_2Se_3:$Sn_{0.5}$ are shifted in the high energy region. The optical transmission T for thin films is determined by the expression:

$$T = \frac{(1-R)^2 \exp(-kd)}{1-R^2 \exp(-2kd)}, \qquad (1)$$

where R - is the optical reflection, k - the absorption coefficient, and d - the thickness of the amorphous film.

In the consideration that the member $R^2 e^{-2\alpha d} << 1$ from the equation (1) the expression for calculation of the absorption coefficient is:

$$\alpha = \frac{1}{d} \ln \frac{(1-R)^2}{T} \qquad (2)$$

The optical band gap E_g for all amorphous films was calculated from the relation:

$$(\alpha\, h\nu)^{1/2} = A(h\nu - E_g), \qquad (3)$$

where A – is a constant. A plot $(\alpha \cdot h\nu)^{1/2} \sim h\nu$ (Tauc plot) yields a straight line and the extrapolation to the photon energy axis $(\alpha \cdot h\nu)^{1/2} \to 0$ give the values of the optical band gap E_g.

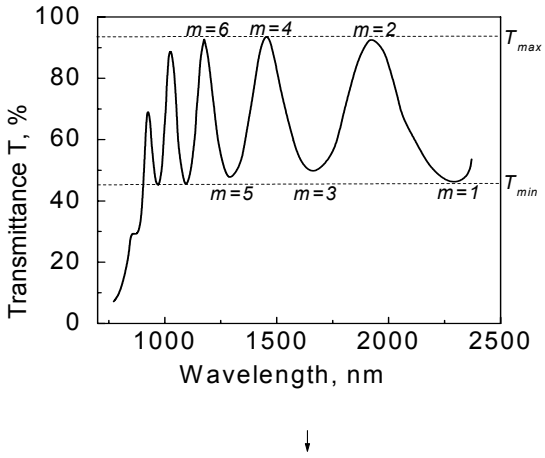

Fig.1. The transmission spectra of as-deposited amorphous Sb_2Se_3 (L=0.8 μm) thin film.

The value of the optical band gap for amorphous Sb_2Se_3 films was obtained E_g=1.3 eV. This value for the optical band gap is in a good agreement with those obtained for the Sb_2Se_3 hollow nanospheres (E_g=1.33 eV) [22], and other published data for amorphous Sb_2Se_3 films (E_g=1.25 eV). Increasing of Sn concentration in Sb_2Se_3 decrease the optical band gap, and for amorphous Sb_2Se_3:Sn_{10} films E_g=1.0 eV.

For the semiconductor transparent thin film the transmission spectra, when the thickness d is comparable with the wavelength λ represents the curve with interference maxima and minima (Fig.1). For normal incident light the dependence of transmission T versus wavelength λ, the refractive index n and the thickness d mathematically can be expressed as [23]:

$$T = \frac{(1-R)^2}{1+R^2-2R\cos\delta}, \qquad (4)$$

were $\delta = \frac{4\pi}{\lambda} nd$ and $R = (\frac{n-1}{n+1})$.

From (4) follow that in the transparence region of the spectra at the wavelengths

$\lambda_{\max} = \frac{4nd}{m}$, m=2, 4, 6, . . . we have the maximums, and at the wavelengths $\lambda_{\min} = \frac{4nd}{m}$, m=1, 3, 5, . . . we have the minimums. Than for each λ_m and λ_{m-1}, corresponding to the neighbor extremes in the transmission spectra, we can calculate the refractive index n:

$$n = \frac{\lambda_m \lambda_{m-1}}{2d(\lambda_{m-1} - \lambda_m)} \qquad (5)$$

In this case, when the refractive index non-linearly depends or has a weak dependence on the wavelength, the determined refractive index has an average value in the region of λ_{m-1} - λ_m. In our method we also take into

account the spectral dependence of the refractive index of the substrate $T_0 = \frac{2n_0}{n_0^{\ 2}+1}$, where n_0 is the refractive index of the substrate. The first approximation of the refractive index (without taking into account the absorption of the thin film) was calculated using the expression:

$$n = \sqrt{\frac{2n_0}{T} - \frac{n_0^2+1}{2} + \frac{\sqrt{-4n_0^2T^2 + (T + Tn_0^2 - 4n_0)^2}}{2T}}, \quad (6)$$

The next approximations of the refractive index were calculated using the expression:

$$T_{extr}^{\ 0} = \frac{T_{\min}}{[1 - A\gamma + (A^2 - B/2)\gamma^2]}, \quad (7)$$

where $T_{\min}$ and $T_{\max}$ are the experimental data, and

$$A = \frac{(n_0^2+n)(n+1)^3 + (n_0^2-n)(n-1)^3}{4(n^2+1)(n_0^2+n^2)}, \quad (8)$$

$$B = \frac{(n_0^2+n)(n+1)^3 - (n_0^2-n)(n-1)^3}{4(n^2+1)(n_0^2+n^2)}, \quad (9)$$

The dispersive curves of the refractive index n for amorphous Sb_2Se_3 films are presented on the Fig.2. Light exposure and heat treatment increase the refractive index for Sb_2Se_3, and for amorphous films doped with Sn impurities.

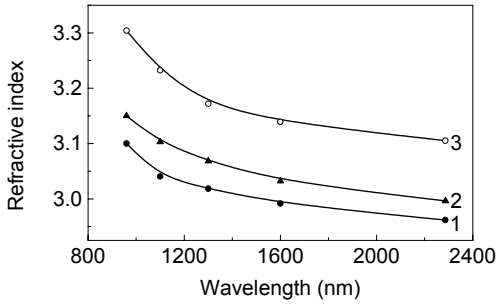

Fig.2. The dispersion curves of the refractive index for amorphous Sb_2Se_3 thin films.
1 – as deposited; 2 – heat treated, 3 – illuminated

Fig.3 shows the dependence of the refractive index *n* versus λ for all investigated amorphous films. The effect of increasing of the refractive index under illumination and heat treatment, as was mentioned above can be used for optical storage devices with high capacities [17-19].

It was shown that the refractive index depends on the Sn concentration in amorphous Sb_2Se_3 films, on light irradiation, and heat treatment. Fig.4 shows the dependence of the refractive index *n* versus Sn concentration for amorphous Sb_2Se_3:Sn_x films. In the wavelengths region 960÷2300 nm tin impurities (up to 0.5 at.% Sn) decrease the refractive index, when for the amorphous films wit tin impurities more than 0.5 at. % Sn the refractive index increases. This may be due to the formation of new structural units, and by the metallization of the atomic bonds.

The maximal modifications of the refractive index Δn (about $\Delta n \sim 0.20$) occur for the composition Sb_2Se_3:$Sn_{0.01}$ and Sb_2Se_3:$Sn_{0.05}$. That allows us to conclude that doping of amorphous Sb_2Se_3 films with small concentrations of tin initiate the photostructural transformations under light irradiation, and make these materials suitable for registration of optical information. The similar effect was observed for the amorphous Sb-Se-In films. Increasing of In atoms in Sb-Se-In films improve the optical information recording characteristics [24]. Fig.5 shows the dependence of modification of the refractive index versus Sn concentration for amorphous Sb_2Se_3:Sn_x films under the light exposure (1) and heat treatment (2).

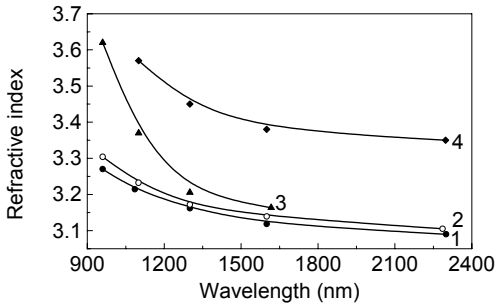

Fig.3. The dispersion curves of the refractive index for amorphous Sb_2Se_3 (1), Sb_2Se_3:$Sn_{0.01}$ (2), and Sb_2Se_3:$Sn_{0.5}$ (3), and Sb_2Se_3:$Sn_{10.0}$ (4) thin films.

To initiate photostructural transformations in thin film samples a He-Ne laser (λ=0.63 μm, *W*=10 mW) was used as a source of light exposure. The splitter was used for divide the laser beam: one Si-photodetector was used for measuring the film transmittance, and another Si-photodetector was used for measuring the time stability of the laser intensity.

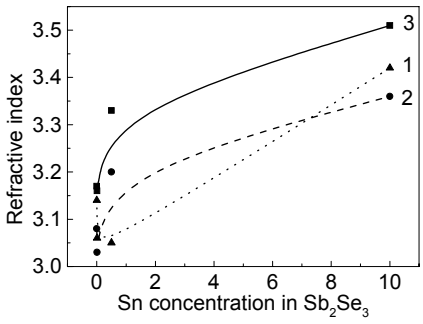

Fig.4. The dependence of the refractive index versus Sn concentration for amorphous Sb_2Se_3:Sn_x thin films. 1 – as deposited; 2 – heat treated, 3 – illuminated

The total transmittance of the film was currently measured during the exposure time with the aid of a registration

module. The experimental set-up included a laser, a digital build-in PC-card for data acquisition PCI-1713A connected with the Si-photodetector. Special software was elaborated for automatic measurements.

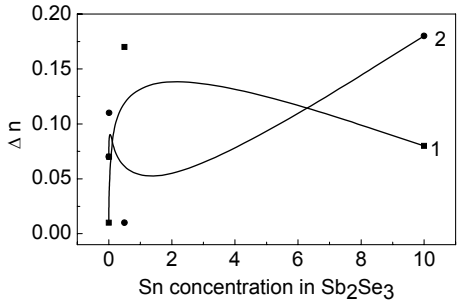

Fig.4. The modification of the refractive index versus Sn concentration for amorphous Sb_2Se_3:Sn_x thin films under illumination (1) and heat treatment (2).

Photocondarkening relaxation was measured during illumination for as-deposited amorphous Sb_2Se_3:Sn_x. Increasing of tin concentration up to 0.5 at.% Sn increase the photodarkening, while for the composition Sb_2Se_3:$Sn_{10.0}$ the photodarkening decrease.

3. Summary

The optical absorption spectra of amorphous Sb_2Se_3 and Sb_2Se_3:Sn thin films were used in order to determine the optical band gap and the refractive index. The modifications of the refractive index under the light exposure and heat treatment also were investigated.

Acknowledgement

This work was supported by the Supreme Council for Science and Technological Development of the Academy of Sciences of Moldova (Project 06.408.012F**)**

References

[1]. A.M.Andriesh, M.S.Iovu, In Series; Optoelectronic Materials and Devices, V.1, 2004, Non-Crystalline Materials for Optoelectronics, Eds. G.Lucovsky & M.Popescu, INOE Publishing House, Bucharest 2004, p.155.
[2]. M.S.Iovu, S.D.Shutov, L.Toth, Physica Status Solidi (b), **195**, 149 (1996).
[3]. M.S.Iovu, N.N.Syrbu, S.D.Shutov, I.A.Vasiliev, S.Rebeja, E.Colomeico, M.Popescu, F.Sava, Physica Status Solidi (a), **175**, 615 (1996).
[4]. M.S.Iovu, S.D.Shutov, V.I.Arkhipov, G.J.Adriaenssens, J. of Non-Cryst. Solids **299&302**, 1008 (2002).
[5]. M.S.Iovu, S.D.Shutov, M.Popescu, J. of Non-Cryst. Solids **299&302**, 924 (2002).
[6]. P.Boolchand, D.G.Georgiev, M.S.Iovu, Chalcogenide Letters **2**, 27 (2005).
[7]. G.Z.Vinogradova, Glass-forming and Phase Equilibrium in Chalcogenide Glasses, Nauka, Moscow (1984) (In Russian).
[8]. N.Kawahashi, H.Shiho, J. Mater. Chem. **10**, 2294 (2000).
[9]. K.Y.Rajapure, C.D.Lokhande, C.H.Bhosele, Thin Solid Films **311**, 114 (1997).
[10]. A.M.Fernandez, M.G.Merino, Thin Solid Films, 1-2, 202 (2000).
[11]. P.Kumar, R.Thangaraj, Solid State Communic., 140, 525 (2006)
[12]. S.Gautam, D.K.Shukla, S.Jain, N.Goyal, J. of Physics 50, 25 (1998).
[13]. Y.Yu, R.H.Wang, Q.Chen, L.-M.Peng, J. Phys. Chem. B 110, 13415 (2006)
[14]. Z.Deng, M.Mansuripur, A.Musat, Nano Letters, 9, 2015 (2009).
[15]. T.Aoki, H.Shimada, N.Hario, N.Yoshida, K.Shimakawa, S.R.Elliott, Phys.rev. **B59**, 1579 (1999).
[16]. S.Jayakumar, C.Balasubramanian, K.Narayandass, D.Lmangalaranj, C.P.Girija Vallabhan, Mater. Res. Bull., **30**, 1141 (1966).
[17]. P.Kumar, R.Thangaraj, J. of Non-Cristalline Solids **352**, 2288 (2006).
[18]. P.Kumar, K.S.Bindra, N.Suri, R.Thangaraj, J. Phys. D: Appl. Phys. **39**, 642 (2006).
[19]. P.Arun, A.G.Vedeshwar, N.C.Mehra, J. Phys. D, Appl. Phys. **32**, 183 (1999).
[20]. A.Guessous, J.Sarradin, P.Papet, K.Elkacemi, S.Belcadi, A.Pradel, M.Ribes, Sensors and Actuators B: Chemical **53**, 13 (1998).
[21]. A.Pradel, O.Valls, C.Cali, G.Taillades, A.Bratov, C.Dominguez, M.Ribes, J. of Optoelectronics and Advanced Materials **3**, 641 (2001).
[22]. Z.Yunxia, L.Guanghai, Z.Bo, Z.Lide, Materials Letters **58**, 2279 (2004).
[23]. Yu.I.Uhanov, Optical properties of semiconductors, Ed. V.M.Tuchkevich, NAUKA, Moscow, 1977 (In Russian).
[24]. V.M.Rubish, P.P.Shtets, V.V.Rubish, D.G.Semak, B.R.Tsizh, J. of Optoelectronics and Advanced Materials 5, 1193 (2003)

Appendix:

$$\gamma = \ln \frac{16n^2 n_0 - [(-1)^m 2(n^2-1)(n_0^2-n^2)] + \sqrt{4(n+1)^3(n_0^2+n)(n-1)^3(n_0^2-n)T^2_{\max} + [(-1)^m 2(n^2-1)(n_0^2-n^2)T_{\max} - 16n^2 n_0]^2}}{2(n+1)^3(n_0^2+n)T_{\max}}$$